



RI		AD-A277 865		E		Form Approved OMB No. 0704-0188	
Public reporting burden for gathering and maintaining collection of information, "Davis Highway, Suite 1204."				Use, including the time for reviewing instructions, searching existing data sources, action. Send comments regarding this burden estimate or any other aspect of this form, Paperwork Reduction Project (0704-0188), Washington, DC 20503.			
1. AGENCY USE ONLY (Leave blank)		2. REPORT DATE Feb 1994		3. REPORT TYPE AND DATES COVERED Final Report 1 Nov 89 - 28 Feb 94			
4. TITLE AND SUBTITLE "Superconducting Meissner Effect Bearings for Cryogenic Turbomachines"				5. FUNDING NUMBERS F49620-90-C-0007 (2)			
6. AUTHOR(S) J. Valenzuela J. Martin				<div style="text-align: center;"> DTIC SELECTED APR 07 1994 S F D </div>			
7. PERFORMING ORGANIZATION NAME(S) AND ADDRESS(ES) Create Incorporated P.O. Box 71 Hanover, NH 03755							
8. PERFORMING ORGANIZATION REPORT NUMBER TM-1650 AFOSR-TR- 94 0135				9. SPONSORING/MONITORING AGENCY NAME(S) AND ADDRESS(ES) Sponsored by: SDIO/IST Monitored by: AFOSR Bolling AFB, DC 20332-0001			
10. SPONSORING/MONITORING AGENCY REPORT NUMBER				11. SUPPLEMENTARY NOTES			
12a. DISTRIBUTION / AVAILABILITY STATEMENT <div style="border: 1px solid black; padding: 5px; width: fit-content; margin: 10px auto;"> This document has been approved for public release and sale; its distribution is unlimited. </div>				94-10514  100420			
13. ABSTRACT (Maximum 200 words) <p>This is the final report of a Phase II SBIR project to develop Meissner effect bearings for miniature cryogenic turbomachines. The bearing system was designed for use in miniature cryogenic turboexpanders in reverse-Brayton-cycle cryocoolers. These cryocoolers are designed to cool sensors on satellites. Existing gas bearings for this application must run relatively warm, so the heat leak from the bearings down the overhung shaft and into the cold process gas imposes a penalty on the cycle efficiency. By using cold Meissner effect bearings, this heat leak could be minimized and the input power per unit of cooling for these cryocoolers could be reduced.</p> <p>Two bearings concepts were explored in this project. The first used an all-magnetic passive radial suspension to position the shaft over a range of temperatures from room temperature to 77 K. This bearing concept was proven feasible, but impractical for the miniature high-speed turbine application since it lacked the required shaft positioning accuracy.</p> <p style="text-align: right;">-Continued on back.</p>							
14. SUBJECT TERMS Meissner-Effect Bearings				15. NUMBER OF PAGES 28			
16. PRICE CODE				17. SECURITY CLASSIFICATION OF REPORT			
18. SECURITY CLASSIFICATION OF THIS PAGE		19. SECURITY CLASSIFICATION OF ABSTRACT		20. LIMITATION OF ABSTRACT			

C 4 6 0 4 3

Abstract-Continued

A second bearing concept was then developed, in which the Meissner effect bearings are combined with self-acting gas bearings. The Meissner effect bearing provides the additional stiffness and damping required to stabilize the shaft at low temperature, while the gas bearing provides the necessary accuracy to allow very small turbine tip clearances (5mm) and high speeds (>500,000 rpm).

AFOSR-TR- 94 0135

DRAFT

Approved for public release;
distribution unlimited.

Superconducting Meissner Effect Bearings for Cryogenic Turbomachines

Phase II Final Report

Javier A. Valenzuela
Jerry L. Martin

Creare Incorporated
P.O. Box 71
Hanover, NH 03755

February 1994

Sponsored by:

Innovative Science and Technology Branch
Strategic Defense Initiative Organization (SDIO/IST)

Prepared for:

Air Force Office of Scientific Research (AFOSR)
Bolling AFB, DC

Accession For	
NTIS CRA&I	<input checked="checked" type="checkbox"/>
DTIC TAB	<input type="checkbox"/>
Unannounced	<input type="checkbox"/>
Justification	
By	
Distribution /	
Availability Codes	
Dist	Avail and/or Special
A-1	

DTIC QUALITY INSPECTED 3

Government Purpose License Rights (SBIR Program)

Contract No. F49620-90-C-0007
Contractor: Creare Incorporated

For a period of two (2) years after delivery and acceptance of the last deliverable item under the above contract, this technical data shall be subject to the restrictions contained in the definition of "Limited Rights" in DFARS clause at 252.227-7013. After the two-year period, the data shall be subject to the restrictions contained in the definition of "Government Purpose License Rights" in DFARS clause at 252.227-7013. The Government assumes no liability for unauthorized use or disclosure by others. This legend, together with the indications of the portions of the data which are subject to such limitations, shall be included on any reproduction hereof which contains any portions subject to such limitations and shall be honored only as long as the data continues to meet the definition of Government purpose license rights.

TABLE OF CONTENTS

	Page
LIST OF FIGURES AND TABLES	iv
LIST OF SYMBOLS, ABBREVIATIONS AND ACRONYMS	v
1. SUMMARY	1
2. PURPOSE AND SCOPE OF PROJECT	2
2.1. Introduction	2
2.2. The Need for Meissner Bearings in Miniature Cryogenic Turbomachines	2
2.3. Phase II Technical Objectives and Approach	3
3. PHASE II RESULTS	4
3.1. All Magnetic Suspension	4
3.1.1. Concept	4
3.1.2. Analysis and Separate Effects tests	6
3.1.3. Proof-of-Concept Tests	12
3.2. Hybrid Gas-Magnetic Bearing	14
3.2.1. Concept	14
3.2.2. Analysis	16
3.2.3. Proof-of-Concept Tests	18
4. CONCLUSIONS AND RECOMMENDATIONS	23
5. REFERENCES	24

LIST OF FIGURES AND TABLES

	Page
Figure 1. Meissner bearing system	5
Figure 2. Calculated and measured magnetization curves for a 1.3 mm thick melt-grown superconductor	7
Figure 3. Magnetic field in a 1.3 mm thick melt-grown superconductor	7
Figure 4. Levitation force for a 25 mm magnet above a melt-grown superconductor—comparison of model and experiment	8
Figure 5. Experimental setup for force data	8
Figure 6. Dynamic stiffness and damping test facility.	9
Figure 7. Amplitude vs. frequency for the normal and superconducting states	10
Figure 8. Meissner bearings breadboard	11
Figure 9. Coastdown curve for 2.5 cm rotor	11
Figure 10. Passive magnetic suspension test article	13
Figure 11. Magnetic field around shaft magnets	14
Figure 12. Hybrid gas/Meissner-effect bearing	15
Figure 13. Hybrid gas/magnetic suspension turbomachine layout	18
Figure 14. Hybrid gas/magnetic suspension turbomachine	19
Figure 15. Hybrid gas/magnetic suspension test facility	20
 Table 1. Gas Bearing Operating Conditions	 17

LIST OF SYMBOLS, ABBREVIATIONS AND ACRONYMS

A	magnetic vector potential ($\mathbf{B} = \nabla \times \mathbf{A}$)
B	magnetic flux density
C	shaft-pad radial gap
J	current density
J_c	critical current density
LN₂	liquid nitrogen
N	speed
T	temperature
T_c	critical temperature
YBCO	Yttrium-Barium-Copper-Oxide superconductor
d	shaft diameter
p_a	ambient pressure
r	shaft radius
Λ	compressibility parameter
μ	viscosity
μ₀	permeability of free space
ρ	density
ω	rotational speed

1. SUMMARY

Infrared sensors on satellites require cooling to achieve high sensitivity and high signal-to-noise ratio. Conventional cooling systems for these sensors use open-cycle cryogen systems. These systems are less desirable for long-duration missions because the weight of the cryogens at launch can become impractically large. For this reason, there has been significant interest in closed-cycle cryocoolers. These cryocoolers use Joule-Thomson, reverse-Brayton, or Stirling cycles to cool the sensor. Key issues for these machines are efficiency (ratio of input power to cooling power), reliability, vibration and system mass.

Creare is currently developing reverse-Brayton cryocoolers which use self-acting tilt-pad gas bearings to support the shaft. These are miniature turbomachines with turbine sizes below 4 mm diameter which operate at speeds approaching 600,000 rpm. The current generation of tilt-pad gas bearings do not operate well at cryogenic temperatures, so the gas bearings are placed in a warm housing at one end of the shaft, and the turbine is cantilevered into the cold stream. This configuration leads to a heat leak into the cold space which subtracts from the available cooling capacity. Since the ratio of input power to cooling power is high, this heat leak leads to a substantial increase in the cryocooler input power per watt of net cooling delivered. We showed in Phase I of this project that incorporating cold bearings into the turboexpander of a reverse-Brayton cryocooler could reduce the specific cycle input power by 40 percent.

One path to cold bearings is to use the Meissner-effect generated by a high temperature superconductor. By employing a combination of permanent magnets in the shaft and superconductors in the housing, a passive Meissner-effect bearing can be produced. The overall objective of this project was the development and demonstration of a turbomachine that employs Meissner bearings for radial support of the shaft.

Two bearing concepts were explored in this project. The first used an all-magnetic passive radial suspension to position the shaft over a range of temperatures from room temperature to 77 K. In this concept, the shaft includes a permanent magnet near each end. These magnets are arranged to set up a radial repulsion between like poles when they interact with annular permanent magnets in the housing. A gas thrust bearing at one end of the shaft provides a stable-non-contact suspension in the axial direction. Superconductors are arranged in the housing close to the ends of the shaft. This arrangement provides a non-contact way of positioning the shaft while the superconductors are above their critical temperature. Once the superconductors are cooled below the transition temperature, the superconductors provide additional stiffness and damping to allow high speed operation. This bearing concept was proven feasible, but impractical, for the miniature high-speed turbine application since it lacked the required shaft positioning accuracy.

A second bearing concept was then developed, in which the Meissner-effect bearings are combined with self-acting gas bearings. Previous studies had shown that the stability of tilt-pad gas bearings was reduced at low temperatures. In the hybrid gas-magnetic bearing, the Meissner-effect provides additional stiffness and damping to help stabilize the shaft at low temperature, while the gas bearing provides the necessary accuracy to allow very small turbine tip clearances (5 mm) and high speeds (>500,000 rpm). A proof-of-concept test article was fabricated and tested. These tests showed only a small improvement in performance over gas bearings alone. The improvement was not sufficient to allow high speed operation. We conclude that this concept is also not practical for high-speed miniature turbomachines.

2. PURPOSE AND SCOPE OF PROJECT

2.1. Introduction

This is the final report for the project entitled "Superconducting Meissner-effect Bearings for Cryogenic Turbomachines". The program was aimed at the development of a Meissner bearing system for miniature cryogenic turboexpanders used in Brayton cycle cryocoolers. This research was sponsored by the Innovative Science and Technology Branch of the Strategic Defense Initiative Organization (SDIO/IST), and managed by the Air Force Office of Scientific Research (AFSOR) under contract F49620-90-C-0007. The Air Force Project Manager was Dr. Harold Weinstock and the Principal Investigator at time of project completion was Dr. Javier Valenzuela. The period of performance for the contract was Nov. 1, 1989 through Feb. 28, 1994.

The project was conducted at Creare Inc. of Hanover, New Hampshire. The Principal Investigators were Dr. V. Iannello and Dr. J.A. Valenzuela. Additional technical contributors were Dr. M.K. Sahm and Mr. M.P. Day, who conducted part of the materials characterization tests, and Dr. J.L. Martin, who led the conceptual design and bearing testing activities. Dr. P.J. Magari and Mr. W.H. Affleck performed the mechanical design of the test facility.

This report is organized into four sections. Section 2 provides background material and summarizes the Phase II objectives and technical approach. Section 3 describes the results of the Phase II research. Finally, the main conclusions of the work are summarized in Section 4.

2.2. The Need for Meissner Bearings in Miniature Cryogenic Turbomachines

Spaceborne infrared sensors for surveillance and intelligence gathering require cryogenic cooling to achieve high sensitivity and high signal to noise ratio. Conventional open-cycle systems rely on the boil-off of either liquid or solid cryogens. However, such systems become less desirable for extended duration missions, since the cryogen mass at launch becomes impractically large. For these long duration missions, active cryocoolers are under development. These cryocoolers use either Stirling or reverse-Brayton cycle refrigerators to cool the focal plane. A key issue in the design of these machines is their efficiency, usually expressed as the number of watts of input power per watt of net cooling. Since this ratio of input power to cooling power is large, small parasitic conduction losses at the cold end translate into large increases in input power and mass. To minimize the radiator mass and the power required by the cooler, the efficiency must be maximized.

Creare is currently developing reverse-Brayton cryocoolers employing self-acting gas bearings to support the turboexpander shaft. These bearings need to run relatively warm, since their load capacity and damping relies on temperature-dependent gas viscosity. In a practical design, this means the bearings run warm, while the turbine is cantilevered into the cold stream. The temperature difference between the warm end of the shaft and the cold end results in a parasitic heat leak down the shaft and into the gas, decreasing the cooler's efficiency. The relative significance of this effect increases as the cooling capacity decreases; a practical lower limit for cooling power using current technology is in the range of 3 to 5 watts.

If the warm gas bearings could be replaced with bearings running at cryogenic temperatures, then the efficiency of a cryocooler could be greatly increased. In Phase I, we showed analytically that a 40 percent decrease in specific input power could be achieved by incorporating Meissner-effect bearings. These studies were performed for a 1 watt, 10 K cryocooler, where warm gas bearings for the coldest turboexpander were replaced with Meissner bearings.

Meissner-effect bearings have several advantages for turboexpanders:

- they are non-contact bearings, not subject to wear,
- they impose minimal drag on the shaft,
- they do not require an external power supply,
- they do not require a control system.

Meissner-effect bearings could also find application in terrestrial applications where the passive nature and low drag of the bearings offset the need for cryogenic coolants.

2.3. Phase II Technical Objectives and Approach

The overall objective of Phase II was the development and demonstration of a turbomachine that employs Meissner bearings for radial support of the shaft. In Phase I, we determined analytically that Meissner bearings are feasible for incorporation into turboexpanders. We also showed that present manufacturing techniques used for ceramic superconductors could be employed in a Meissner bearing design.

The specific technical objectives of the Phase II program were to:

- Fabricate a Meissner bearing test apparatus and generate data from which advanced analytical models could be developed and a final bearing design could be specified.
- Design and fabricate a Meissner-effect bearing system appropriate for use in small cryogenic turbomachines.

The technical approach originally focused on the development of a completely passive magnetic suspension. This bearing system was developed through a combination of analytical modeling, separate effects testing and fabrication and testing of proof-of-concept hardware. The testing showed that this concept would not yield a practical turboexpander, so the development effort shifted to a more promising concept which combines some of the best features of gas bearings and Meissner-effect bearings. This concept was developed through a combination of separate effects testing and fabrication of proof-of-concept hardware.

3. PHASE II RESULTS

This section describes the results of the Phase II development effort. The first part describes the development of the all-magnetic suspension, while the second part describes the development of a hybrid gas-magnetic bearing.

3.1. All Magnetic Suspension

The goal of the development effort was to conceptualize and fabricate a Meissner-effect bearing system for a miniature turbomachine. The challenging element of this task was to design a Meissner bearing system that precisely positions the shaft so that small running clearances are possible in the turbine, resulting in low leakage rates around the turbine blade passages. Another challenge was the development of a means to support the shaft while the superconductor is cooled below its critical temperature (T_c). Because of the hysteretic nature of Type II superconductors, a range of equilibrium positions for the shaft exists. A shaft that starts off in mechanical contact with a non-rotating member must therefore be lifted off by some other means, be it manually or otherwise. In the past, this has limited Meissner bearings to use in laboratory demonstrations and basic research devices. As such, the bearing has little practical use.

During this project, an improved superconducting bearing was developed that removed this limitation. By employing a special configuration of permanent magnets and supplying the bearing with a small supply of gas, the shaft could be stably and precisely positioned at all times.

The bearing offered the following advantages over other passive superconducting bearings. It:

- Non-mechanically positioned the rotating shaft while the superconducting material passed from its normal to superconducting state, thereby "pinning" the magnetic flux such that the shaft was "cradled" in a very precise position.
- Could support steady loads, even when the superconductor exhibited "flux creep".
- Allowed operation of the superconductor in the hysteric Type II regime, where superconductor-magnet forces are highest.
- Provided load capacity and stiffness, even when the superconducting materials are at temperatures above their critical temperatures and are therefore not superconducting.
- Did not require precision machining of the superconducting material.
- Allowed the gap between the permanent magnets and the superconducting materials to be minimized, thereby increasing the stiffness, load capacity, and damping of the bearing.

3.1.1. Concept

The improved bearing is shown in Figure 1. The bearing system consists of permanent magnets in the bore of the shaft; stationary permanent magnets of annular shape which encircle the shaft; superconducting materials at the shaft ends in very close proximity to the shaft magnets; and a duct and pinhole outlet which direct a flow of gas towards one shaft end. As shown in Figure 1, the turbine may be located midway between the bearings.

When the superconductor materials are above their critical temperature and therefore not superconducting, the stationary permanent magnets interact with the permanent magnets in the shaft to radially position the shaft. With the magnet polarities as shown, the magnet configuration will center the shaft in the stationary permanent magnets due to radial repulsive forces between poles of the same polarity. The shaft is stably supported along its radial axes.

The permanent magnet interaction also produces an unbalanced axial force on the shaft so that the permanent magnet suspension is by itself unstable (in accordance with Earnshaw's Theorem). In order to produce stability, a gas jet is directed towards one end of the shaft. The position of the stationary magnets can be chosen to produce a net magnetic force towards the gas jet. This net force is exactly balanced by the force of the gas jet impinging on the shaft. Because the gas jet imparts a force on the shaft with an axial stiffness much greater than the "negative" (unstable) stiffness produced by the permanent magnet, the shaft is stably positioned without mechanical contact. In this suspended position, the shaft may rotate freely about its axis.

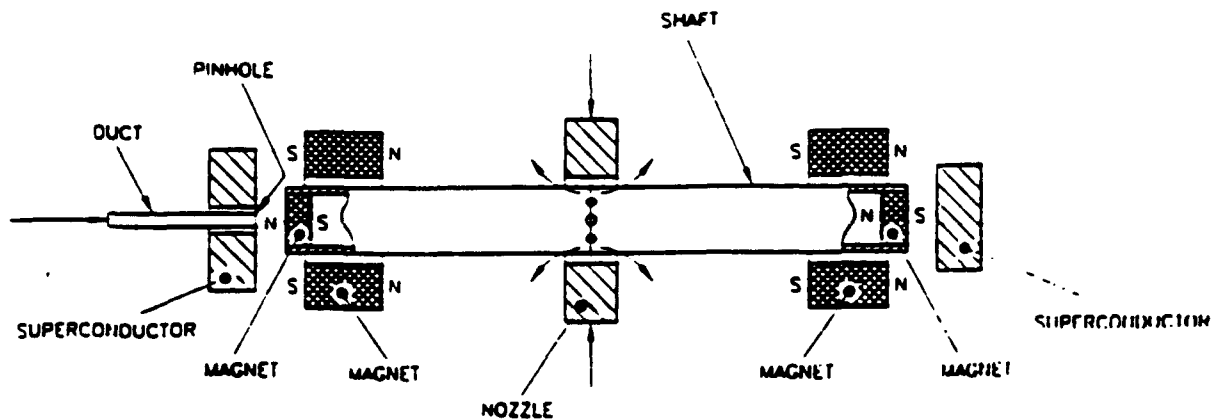


Figure 1. Meissner bearing system

As the superconductors are cooled below their transition temperature, the magnetic flux produced by the permanent magnets that penetrates the superconductor is "pinned". Any change in position of the shaft will induce supercurrents in the superconductor which will tend to resist the change in position. As a result, the shaft will be "clamped" in the desired position. The superconductor-magnet interaction generates a restoring force as the shaft is transversely displaced in any direction away from its equilibrium position. This interaction, however, does not resist shaft rotation, due to the azimuthal symmetry of magnetic field produced by the permanent magnets. The rotational drag can thus be made quite small.

It might appear that the superconductors are not necessary since the permanent magnets and gas jet alone are sufficient for positioning the shaft. In fact, the superconductors greatly add to the stiffness and

damping of the bearing system. Without the superconductors, the bearing would have insufficient stiffness and damping for high speed rotation of the shaft.

Flux creep, or a decay of supercurrent amplitude with time, has been experimentally observed in high temperature superconductors. If a magnet that is "pinned" in a certain position is subsequently displaced, the restoring force generated by the induced currents will initially be high, and then will decay with time. By incorporating the stationary permanent magnets into the bearing system, the bearing will support steady loads even with superconductor flux creep.

Because the interaction between a superconductor and a permanent magnet is maximized at close spacings, the improved bearing offers the advantage of precisely positioning the shaft in close proximity of the superconductor. As a result of the small gap spacing between the superconductor and the face of the permanent magnets in the shaft, the stiffness, damping, and load capacity of the bearing are maximized.

The bearing also offers certain fabrication advantages over other passive superconducting bearings. The superconductor need not be specially contoured or machined. The face of the superconductor need only be ground flat.

Section 3.1.3 describes the test article which was fabricated to test the bearing concept.

3.1.2. Analysis and Separate Effects tests

In order to design bearings which implemented the all-magnetic suspension, we developed analytical models were developed to predict the forces between permanent magnets and superconductors. These models were then verified through a series of separate effects tests.

Critical state model. The first step towards designing the Meissner-effect bearing was the development of sound design methods to optimize the configuration of the Meissner bearings for maximum levitation force and stiffness. To accomplish this, analytical models were developed based on first principles with constitutive relations for superconductor properties such as the current density J_c . The model was compared with experimental force data obtained at Creare.

A one-dimensional magnetization model was first developed to predict the net magnetization of a superconductor when subjected to an external field. Magnetization curves are often known for a superconductor sample from magnetometer measurements, but critical current densities are often not known because of the experimental difficulty of taking the measurement. The 1-D model therefore provides a simple method for "backing out" the current densities when otherwise not known.

The magnetization model is based on Bean's critical state model, which assumes currents in the superconductor are either at their critical density at a given location or are not flowing. The field in the superconductor is thus given by

$$\frac{dB}{dx} = \mu_0 J_c \quad (1)$$

where B is the magnetic field and μ_0 is the permeability of free space. In the Bean model, J_c is assumed constant so that B changes linearly in the superconductor. Here, we allow $J_c(B)$, which more accurately represents HTSCs.

Figure 2 compares the experimental and calculated magnetization curves for a 1.3 mm thick superconductor when the external field is applied along the *c*-axis (conduction in the *a*-*b* plane). The YBCO sample was fabricated and magnetically characterized by Catholic University. It was found that excellent agreement between the experiment and calculations could be obtained with J_c given by

$$J_c = J_0 e^{-|B/B_0|} + J_1 e^{-|B/B_1|} \quad (2)$$

and $J_0 = 1600 \text{ A/cm}^2$, $B_0 = 0.1 \text{ T}$, $J_1 = 3760 \text{ A/cm}^2$, and $B_1 = 100 \text{ T}$. The local magnetic flux densities in the superconductor are shown in Figure 3 for various points on the magnetic hysteresis curves.

A 2-D numerical code was next developed to predict the force between permanent magnets and superconductors in arbitrary geometries. At the heart of this numerical code is a Maxwell's Equations field solver for the vector potential, A , defined by $B = \nabla \times A$.

The permanent magnet is modeled as equivalent surface currents necessary to produce an identical volume magnetization. This assumption assumes uniform magnetization of the magnet (which is valid for rare-earth magnets). The magnet model also includes the demagnetization curve of the hard magnetic material so that the field produced by the magnet is a function of the net reluctance of its environment.

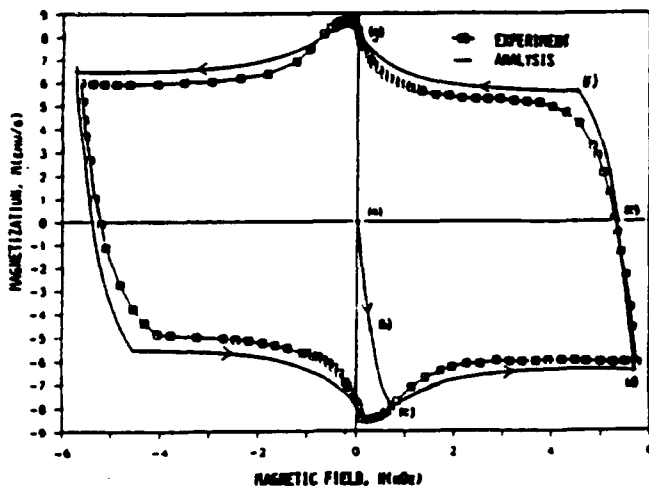


Figure 2. Calculated and measured magnetization curves for a 1.3 mm thick melt-grown superconductor

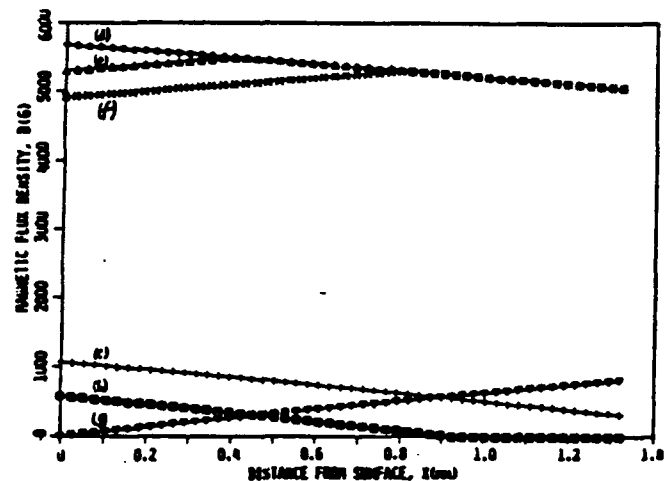


Figure 3. Magnetic field in a 1.3 mm thick melt-grown superconductor

The superconductor is treated according to the critical-state model. In this model, the persistent currents that shield the interior from the applied magnetic fields have a current density equal to the critical current density J_c . The penetration of the magnetic field into the superconductor occurs as follows. Initially, the flux density B equals zero inside the superconductor. On the application of an external field, a shielding

The superconductor is treated according to the critical-state model. In this model, the persistent currents that shield the interior from the applied magnetic fields have a current density equal to the critical current density J_c . The penetration of the magnetic field into the superconductor occurs as follows. Initially, the flux density B equals zero inside the superconductor. On the application of an external field, a shielding current develops in a thin layer on the superconductor surface. If the current density is greater than J_c in this layer, the layer goes normal, i.e., has a finite resistivity and therefore a finite electric field. The presence of the electric field accelerates electrons in the superconductor adjacent to this layer so that the current carrying layer (and magnetic flux) penetrates deeper into the superconductor. This process stops only when the current carrying layer expands sufficiently for the shielding current density to fall just below J_c . Then, instantaneously, the electric field vanishes and the shielding current flows persistently at J_c in the superconductor region it has penetrated.

Once the magnetic field and current densities within the superconductor are known, the Lorentz forces can be calculated in a relatively straightforward manner. Figure 4 compares the experimental force data with the numerical prediction for a 2.5 mm (0.1 in.) cylindrical magnet above a melt-grown superconductor supplied by Catholic University. The only constitutive relations used were the demagnetization curve of the magnet as supplied by the magnet vendor, and the critical current density of the superconductor (Eq. 5). As shown in the figure, the agreement is excellent except at small magnet-superconductor spacings. The setup used to obtain the experimental data is shown in Figure 5.

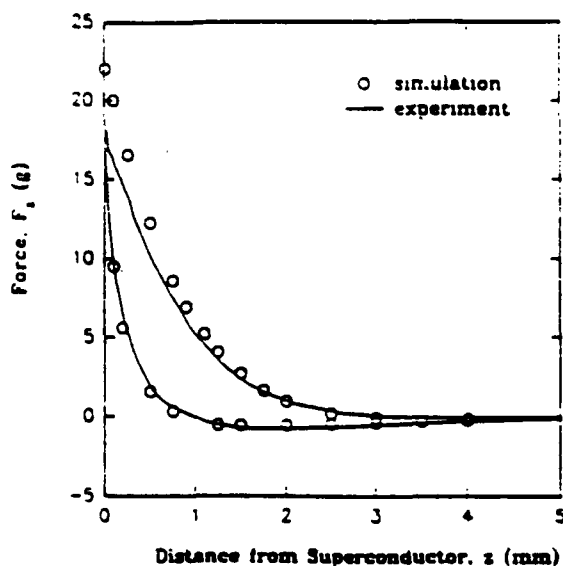


Figure 4. Levitation force for a 25 mm magnet above a melt-grown superconductor comparison of model and experiment

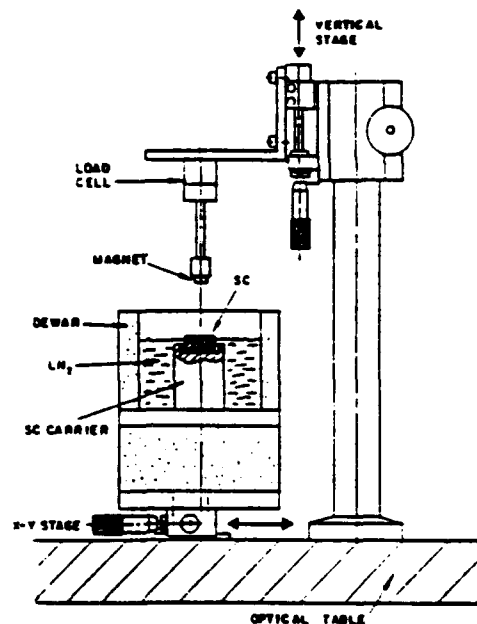


Figure 5. Experimental setup for force data

Stiffness and damping tests. Following these tests, an experiment was designed to give more information on the performance of Meissner-effect bearings. This experiment involved the construction of a test facility which allowed the measurement of the bearing stiffness and damping at small gaps and high frequencies. This facility is illustrated in Figure 6.

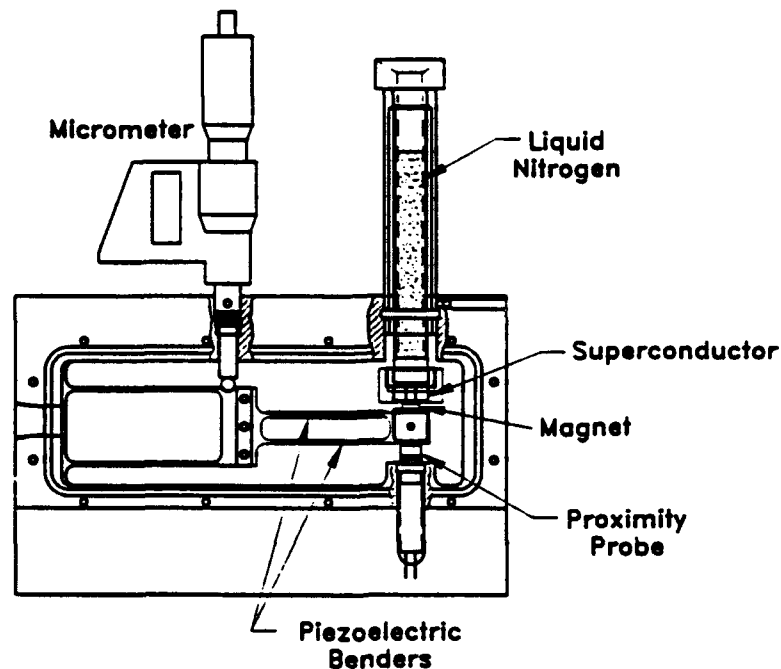


Figure 6. Dynamic stiffness and damping test facility.

The facility consisted of a vacuum chamber housing a piezoelectric bender with a magnet on its free end. A superconductor sample was attached to a small dewar directly above the magnet. By applying a sinusoidal voltage to the piezoelectric elements, the magnet could be moved closer or further away from the superconductor. A micrometer allowed the separation between the magnet and the superconductor to be set. An inductive position sensor measured the magnet position.

Figure 7 shows typical results from this facility. The two curves were obtained by driving the piezoelectric benders with a swept sine wave while recording the amplitude of the vibration. The vibration amplitude increases near the natural frequency of the vibrating beam. This natural frequency is determined by the series combination of the beam stiffness and the stiffness of the Meissner-effect bearing formed by the magnet and the superconductor. The damping of the system can be determined from the width of the resonance peak. Small values of damping lead to narrow resonance peaks, large values to wider peaks. As Figure 7 shows, lowering the temperature of the superconductor below T_c causes the resonance peak to shift to higher frequencies and to broaden, showing that the Meissner-effect bearing provides both stiffness and damping, even at these small displacements.

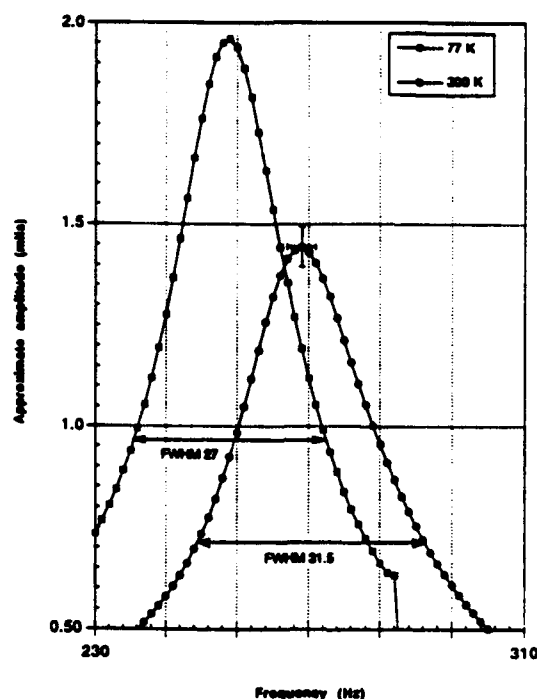


Figure 7. Amplitude vs. frequency for the normal and superconducting states

High speed rotation tests. These tests were intended to demonstrate that rotational and surface speeds prototypical of miniature turbomachines could be stably and repeatably achieved with Meissner-effect bearings. To this end, we fabricated a breadboard design, a simple rotor disk-superconductor configuration.

The simple rotor disk configuration is shown schematically in Figure 8. A cylindrical superconductor approximately 2.5 cm (1.0 in.) in diameter and height was supported in an insulated pool of liquid nitrogen (LN_2). The YBCO superconductor was supplied to Creare by Catholic University, where it was fabricated from a melt-grown process developed by Dr. Hamid Hojaji of the Vitreous State Laboratory. The magnetic rotors for this configuration were rare-earth permanent magnets of cylindrical geometry. Both Nd-Fe-B and Sm-Co materials were tested.

In order to rotationally drive the rotor, two opposed nitrogen jets were tangentially directed at the surface of the magnet at diametrically opposite locations. The two jet configurations served to reduce the net radial jet force on the disk. Two techniques were employed to measure the rotational speed. For the first, a timing mark was painted on the upper face of the rotor, and a strobe was used to determine the rotational speed. This technique was successfully used, but did not allow the determination of rotational speeds during spin-up and coastdown of the rotor. For the second, a timing mark was painted on the side of the disk and detected by an optical sensor. The optical sensor combined the source light-emitting diode (LED) and photo detector in one package. The signal output from the photo detector was fed to conditioning electronics, and then to an oscilloscope, where the waveform consisted of a periodic series of spikes. The frequency of these spikes corresponded to the frequency of rotation of the rotor.

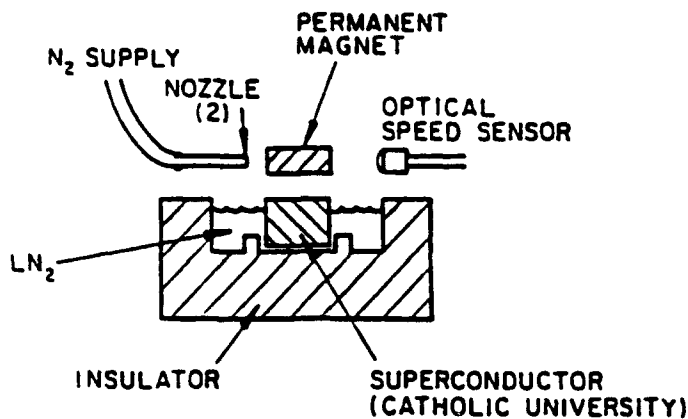


Figure 8. Meissner bearings breadboard

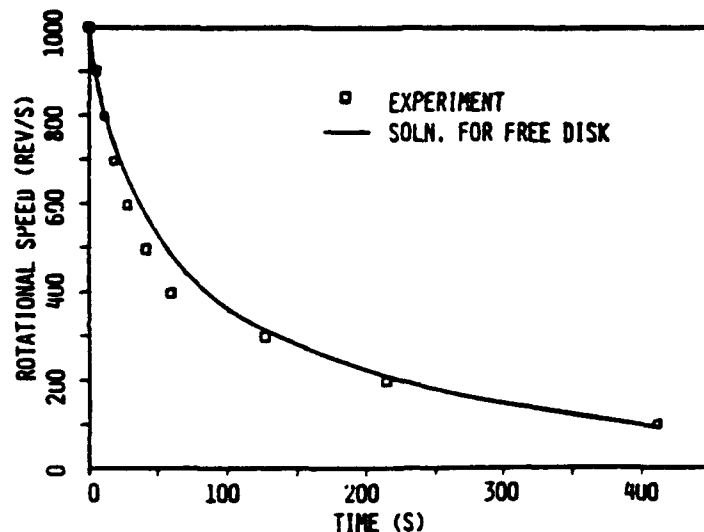


Figure 9. Coastdown curve for 2.5 cm rotor

Using this setup, rotors with diameters between 2.5 and 25 mm (0.1 to 1.0 in.) were rotated to high speeds. In the first set of tests, a Nd-Fe-B rotor with dimensions 25 mm OD x 6.3 mm H (1.0 in. OD x 0.25 in. H) was spun to 60,000 rpm (1000 rev/s), which represented a surface speed of 80 m/s. Once at 60,000 rpm, the gas supplied to the nozzles was stopped, and the rotor coasted down. This coastdown is shown in Figure 9.

If the Meissner bearings are to be used for miniature turbomachines, it is important that the rotational drag they introduce is small compared to the other drag forces acting on the disk, such as windage (aerodynamic drag). To show this, the coastdown of a free disk subjected exclusively to windage was analytically predicted, and this result was compared to the experimentally observed coastdown.

The turbulent drag torque acting on both sides of a free-spinning disk is given by [1]

$$2M = 0.073 \rho \omega^2 R^5 (v/\omega R^2)^{0.2} \quad (3)$$

where ρ is the fluid density, ω is the angular velocity, R is the disk radius, and v is the kinematic viscosity. The coastdown of the disk is governed by

$$2M = I \dot{\omega} \quad (4)$$

where I is the moment of inertia of the disk (which equals $MR^2/2$). After combining (3) and (4), solving for $\dot{\omega}$, and integrating, the following coastdown curve is obtained:

$$\omega = \left[\frac{1}{\frac{1}{\omega_0^{0.8}} + \beta t} \right]^{1.25} \quad (5)$$

where $\beta = 0.058 R^4 \cdot 60 \cdot 2/I$ and ω_0 is initial angular velocity.

Figure 9 compares the analytical windage with the experimental coastdown curves. The agreement is satisfactory for the seven minute coastdown. We conclude, therefore, that the superconductor imparts little additional drag on the rotor.

Further testing was performed with smaller rotors to demonstrate stability at ultra-high rotational speeds. A 6.4 mm (0.25 in.) rotor was spun to a rotational speed of 450,000 rpm (7500 rev/s), which represents a surface speed of 150 m/s. This stable surface speed far exceeds that required by the turboexpander application (about 90 m/s).

3.1.3. Proof-of-Concept Tests

Following the separate effects tests a proof-of-concept test article was fabricated. This test article is shown in Figure 10. The test article consisted of a shaft with an integral impulse turbine, and a housing which contained the turbine nozzles, the permanent magnets, and the gas thrust bearing. The 6.35 mm diameter shaft contained one Nd-Fe-B magnet at each end. A micrometer attached to the thrust bearing allowed the shaft to be positioned axially inside the fixed annular magnets to achieve a stable radial suspension. The superconductors were located in the housing facing the axial ends of the shaft. One superconductor included a small hole for the thrust bearing. The housing was provided with flow passages for liquid nitrogen to cool the superconductors.

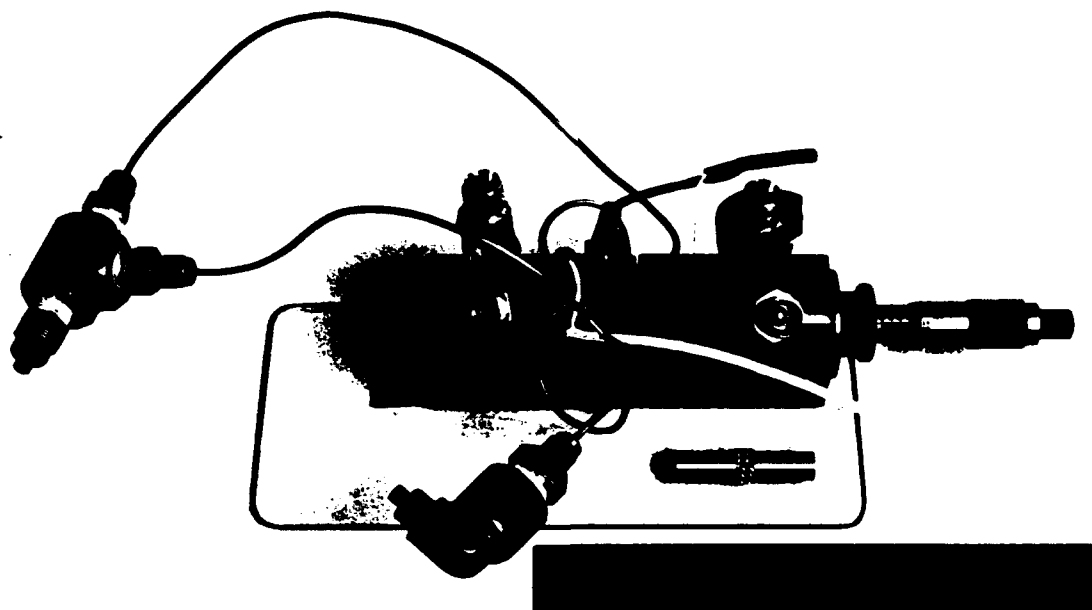


Figure 10. Passive magnetic suspension test article

During operation, capacitance probes monitored the position of the shaft within the bearings. The shaft was placed within the housing and the thrust bearing flow and position were adjusted until the shaft was suspended stably without contact. Helium from a gas bottle was used to drive the impulse turbine. After the shaft was spinning, liquid nitrogen was introduced into the chamber surrounding the test article, and cold nitrogen vapor was passed through the spaces around the superconductors.

The facility was operated at room temperature at speeds of up to 50 rps (3000 rpm). Operation beyond this speed was not possible due to conical mode vibrations of the shaft. Further investigation showed that these vibrations are caused by an offset between the shaft center of mass and the center of the magnetic field. The passive magnetic bearings try to force the shaft to rotate around its magnetic center. Due to variations in the uniformity of the magnets inside the shaft, this magnet center is displaced from the shaft center. Figure 11 illustrates this effect. The figure shows a map of the magnetic field strength around the shaft. These measurements were made by rotating the shaft in the chuck of a precision lathe while measuring the magnetic field strength with a Hall effect probe.

The offset in the magnetic and mass centers of the shaft leads to unbalanced forces on the shaft when it rotates. These unbalance forces, combined with the low intrinsic damping of the passive magnetic suspension, lead to large amplitude excursions at the critical frequencies of the bearing. Even with the large gaps between the magnets and shaft used in the proof-of-concept rig (1.0 mm radial), the shaft was unable to pass through the criticals of the bearing at room temperature.

One approach to reducing the anisotropy of the magnetic field was investigated. In this approach, the single magnets at each end of the shaft were replaced with a stack of four magnets with the same total axial length. By orienting each of the magnets within this stack in such a way as to cancel the individual variations in magnetic field strength, a more uniform magnetic field was achieved in the azimuthal

direction. By using this technique, we were able to reduce the variation in magnetic field around the magnets to well under 1 percent.

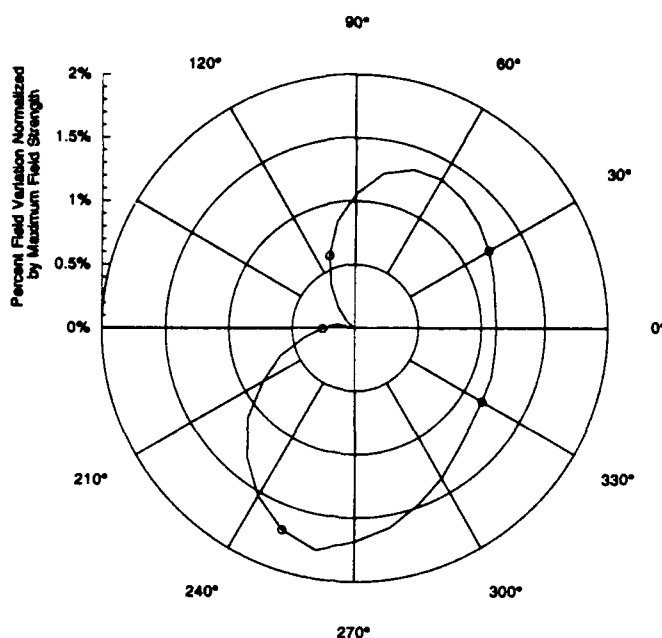


Figure 11. Magnetic field around shaft magnets

A shaft incorporating the aligned magnet stacks was fabricated and tested. Higher speeds were achieved with this configuration, but it was still not possible to pass through the bearing critical speeds. The facility was then cooled to liquid nitrogen temperature. Runout decreased when the superconductors passed through their critical temperatures, and preliminary tests showed that damping was improved. Nonetheless, the runout was excessive for a practical turbomachine, and we abandoned this approach as unfeasible.

These tests verified the basic principle of the bearing system. While this system was capable of supporting and centering the shaft over a range of temperatures, it did not have sufficient stiffness for high speed cryogenic turbines, which require very small tip clearances (on the order of 5 μm) for high efficiency. Since the bearings are not very stiff, any residual unbalance in the shaft leads to large amplitude vibrations at the critical speeds. While the passive magnetic suspension system might be applicable to larger shafts at lower speeds, we conclude that the passive magnetic suspension will not be applicable for miniature, high speed turbomachines.

3.2. Hybrid Gas-Magnetic Bearing

3.2.1. Concept

In order to work around the problems with the non-uniform magnetic field and low stiffness, a new bearing configuration was conceived to provide stable suspension at both cryogenic and ambient temperatures. This bearing is shown in Figure 12. The bearing uses tilt-pad hydrodynamic gas bearings to support the shaft at room temperatures. Tilt-pad gas bearings are well-developed and are used in small turboexpanders produced by Creare. While they have demonstrated excellent performance near room temperature, supporting shafts at well above 600,000 rpm, their performance degrades at low

temperatures. Investigations into the stability of these bearings at low temperatures indicates that the stability degrades due to a combination of the reduction in stiffness and damping at low temperatures. Meissner-effect bearings can provide the additional stiffness and damping required to stabilize the shaft at low temperatures.

The combination of Meissner-effect and self-acting gas bearings could provide a solution to the dilemma which has plagued many researchers in the superconducting bearing field—the same applications which lend themselves to Meissner-effect bearings (small, high speed systems), usually require a level of accuracy in positioning the shaft which cannot be achieved using the Meissner bearings alone. By combining the excellent room-temperature performance and shaft positioning accuracy of gas bearings with the low-temperature stiffness and damping available from the superconductors, a bearing may be constructed which provides both accurate positioning and robust operation at low temperatures.

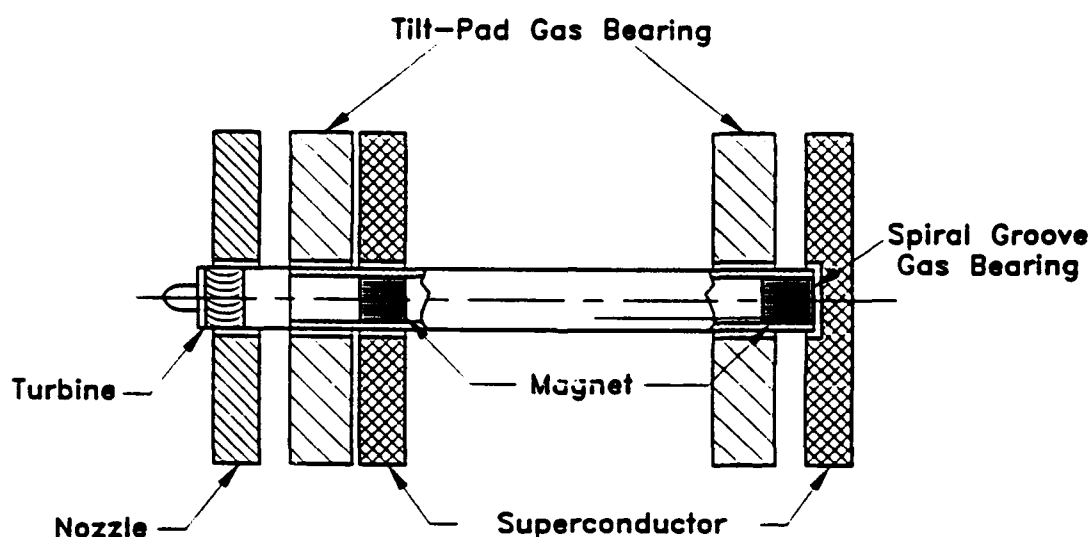


Figure 12. Hybrid gas/Meissner-effect bearing

The improved bearing system is essentially a combination of a hydrodynamic gas bearing and a Meissner-effect bearing. Hydrodynamic gas bearings are used on a number of small high-speed devices including gyroscopes and small turboexpanders. These bearings rely on the viscous pumping of gas between moving surfaces to produce the pressure needed to support the shaft. Creare uses tilting-pad gas bearings on small turbomachines of up to 25 mm in diameter. On our smallest turboexpanders (3 mm diameter), these bearings operate at shaft speeds exceeding 600,000 rpm.

Gas bearings have some disadvantages for cryogenic operation. Since the bearings rely on viscous pumping to develop load capacity, their performance degrades at low temperatures, due to a reduction in gas viscosity. Tests at Creare have shown that the maximum speed for stable bearing operation decreases with temperature. For these reasons, the bearings on our turbomachines typically run relatively warm, while the expander is cantilevered into the cold stream.

Some researchers have attributed the reduction in maximum stable speed for gas bearings at low temperature to the reduction in bearing stiffness brought on by decreased viscosity. As we show below, this may not be strictly true. For the operating points of Creare's tilt-pad gas bearings, the bearing stiffness is fairly insensitive to the gas viscosity since the bearings are operating in a range where compressibility is important.

3.2.2. Analysis

The load capacity of gas bearings depends strongly on the effects of compressibility in the gap. At low speeds and moderate atmospheric pressures, the pressure rise in the gap is small compared to the atmospheric pressure, and the bearing may be analyzed using incompressible assumptions. As speed increases or the bearing operating pressure decreases (on a high-altitude aircraft, for example), the effects of compressibility become important.

The effect of compressibility is typically expressed as a function of the compressibility parameter, Λ .

$$\Lambda = \frac{6\mu\omega r^2}{p_a C^2} \quad (6)$$

where

- μ is the dynamic viscosity,
- ω is the rotational speed in rad/s,
- r is the shaft radius,
- p_a is the atmospheric pressure,
- C is the shaft-pad radial gap.

For values of Λ less than 1, the bearing performance may be adequately predicted by incompressible theory. In this range, the load capacity depends strongly on the value of Λ . Since the viscosity of gases decreases with temperature, the load capacity decreases with temperature for $\Lambda < 1$.

As Λ increases from 1, the slope of the load-capacity vs. Λ curve decreases. For the typical design point for our turboexpander bearings, doubling Λ from 6 to 12 gives only a 20 percent increase in load capacity. Beyond $\Lambda=10$ or so, the load capacity may be considered independent of Λ . This means that the load capacity becomes independent of shaft speed. The only effects of temperature are the variation in viscosity and the possible differential expansion of the shaft and the bearing. For titanium shafts in a Be-Cu bearing, the gap at 100 K is approximately half of that at room temperature. This decrease in gap tends to compensate for the decrease in viscosity, with the net effect being to keep Λ large and the load capacity high. As shown in Table 1, Λ is greater than six at temperatures as low as 80 K for a typical expander design.

Table 1. Gas Bearing Operating Conditions

neon viscosity	μ	1.18E-05	kg/(m-s)
speed	N	7000	rps
angular frequency	ω	43982	rad/s
shaft diameter	d	4.76E-03	m
shaft radius	r	2.38E-03	m
ambient pressure	p	1.01E+05	Pa
radial clearance	C	5.08E-06	m
temperature	T	80	K
compressibility parameter	Λ	6.76	

Creare has performed a number of tests with cold gas bearings. A small bearing test rig was manufactured and used to test tilt-pad bearings with both stainless steel and titanium shafts. The performance of the bearings was measured by determining the speed at which unstable whirling began. At room temperature, this was in the 10,000-12,000 rps range. For the titanium shaft, the whirl onset speed was relatively independent of temperature until about 150 K, when it dropped off rapidly to about 6000 rps at 130 K and then decreased more slowly to 4000 rps at 100 K.

Since the above analysis shows that the bearing stiffness varies only a small amount over this temperature range, we ascribe the decreased stability to decreased damping. As a class, gas bearings exhibit little damping, with perhaps the only significant sources of damping being squeeze-film damping in the gap and any structural damping in the bearings. The first of these damping sources is dependent on the gas viscosity, and therefore will decrease with decreasing temperature. If additional damping could be generated at low temperatures, the region of stable operation could be extended.

High temperature superconductors can provide the additional damping needed to stabilize the bearing. Takahata [3] has shown that a high-temperature superconducting bearing could provide up to 5 N-s/m of damping. Calculations indicate that the tilt-pad bearings require a minimum of 3-4 N-s/m of damping for stable operation. It appears, therefore, that by combining the gas bearing with a Meissner-effect bearing/damper, that the gas bearing could be stabilized at cryogenic temperatures.

Figure 12 shows the hybrid gas/Meissner-effect bearing. The tilt-pad gas bearings are the same as those used in other small high-speed systems. The shaft, however, contains a small magnet mounted inside the shaft near each of the gas bearings. High-temperature superconductors are located at the same axial locations as the magnets. As the shaft is displaced from the center of the bearing, the magnetic field at the surface of the superconductor varies. The resulting changes in the current distribution inside the superconductor dissipate energy, so the superconductors act to damp oscillations. In addition, the superconductor/magnet combination will supply some stiffness to the hybrid bearing.

3.2.3. Proof-of-Concept Tests

In order to test the hybrid bearing concept, we fabricated a small turbomachine incorporating both tilt-pad gas bearings and Meissner-effect radial bearings. Figures 13 and 14 show the turbomachine. The experimental apparatus is shown schematically in Figure 15 and consists of the turbomachine assembly, a base plate, several heat transfer coils and various instrumentation and controls. The entire apparatus is inserted in an insulated container which can be filled with liquid nitrogen to the desired level.

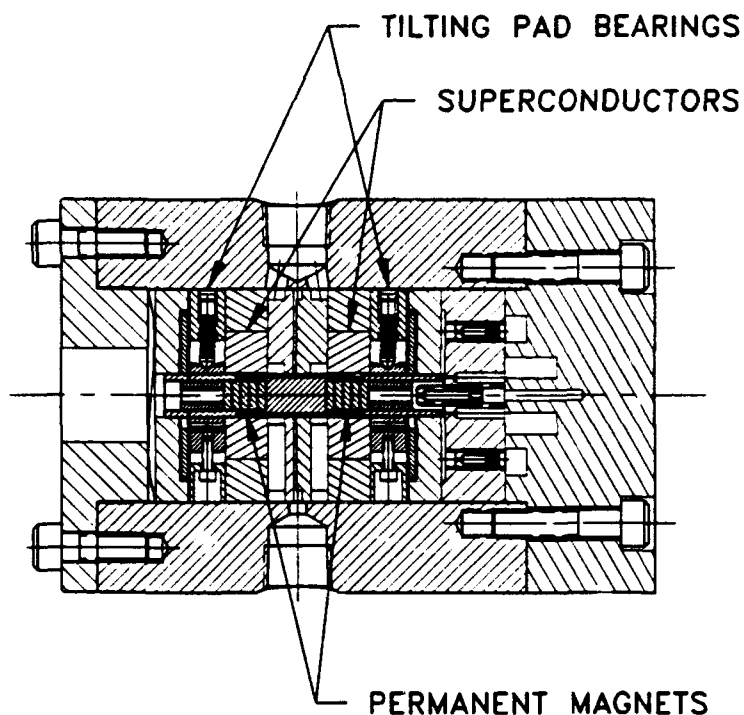


Figure 13. Hybrid gas/magnetic suspension turbomachine layout

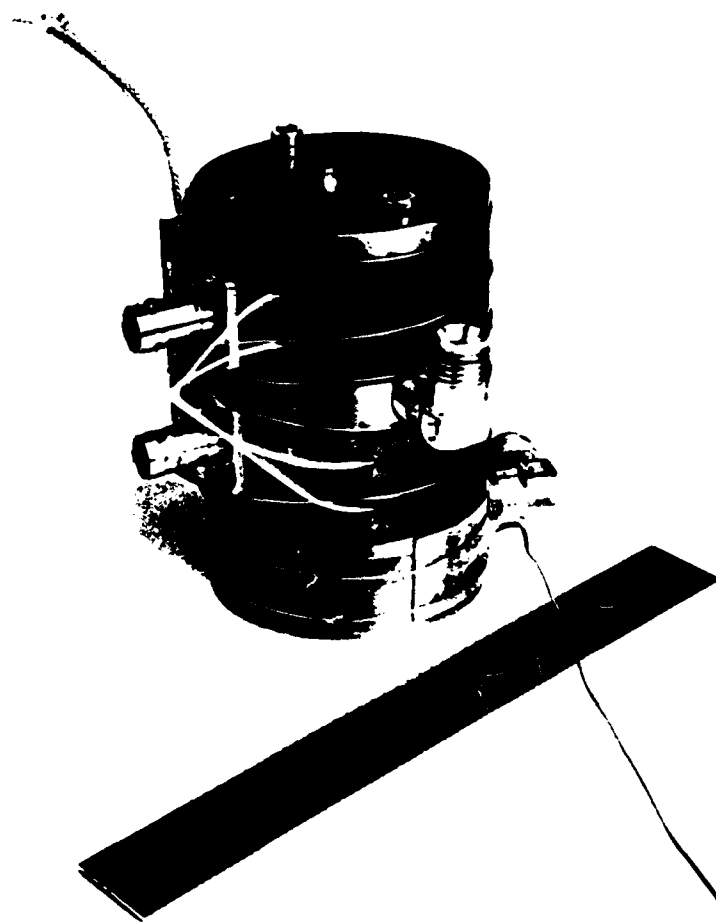


Figure 14. Hybrid gas/magnetic suspension turbomachine

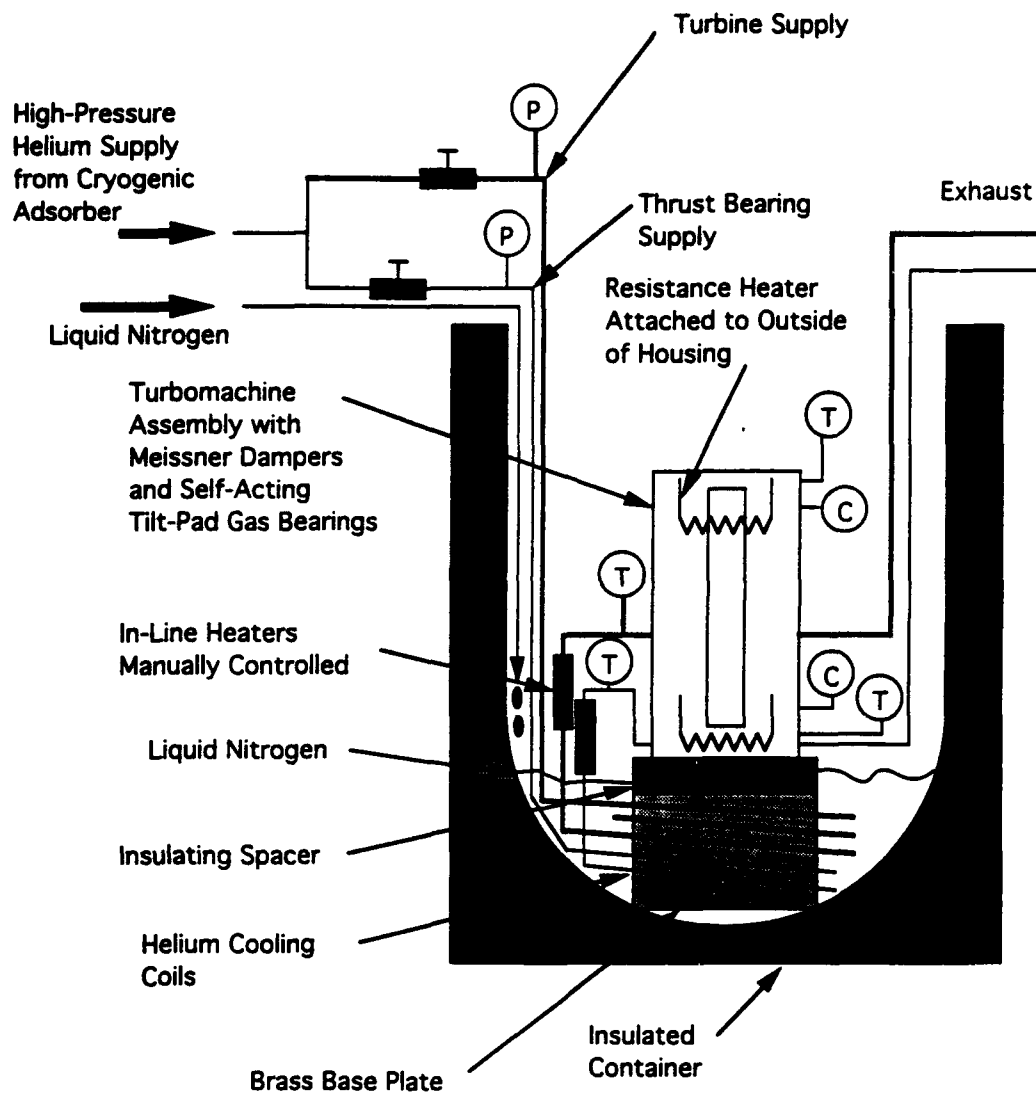


Figure 15. Hybrid gas/magnetic suspension test facility

The turbomachine assembly rests on an insulating base which is immersed in a pool of liquid nitrogen. Electrical resistance heaters are attached to the outside of the housing to provide a moderate level of control over the housing temperature. The housing temperature is monitored at several points on the outer surface via thermocouples. Shaft run-out is monitored via two radial capacitance proximity probes located near each end of the shaft. The capacitance probe outputs are monitored and recorded on a digital oscilloscope and a spectrum analyzer.

The high-pressure helium gas is supplied from a standard pressurized bottle. Supply pressures are monitored via Bourdon tube pressure gauges. The gas is passed through a cryogenic adsorber to remove any contaminants which could potentially freeze out in the turbomachine at liquid nitrogen temperatures. After passing through the adsorber, the thrust bearing and turbine helium gas supplies flow through separate coils which are immersed in the pool of liquid nitrogen. After passing through the coils, the two gas supply lines pass through individual in-line heaters which provide a means for controlling the temperature of the supply streams. Power input to the heaters is varied manually via variable voltage supplies, and the gas temperatures are monitored with thermocouples placed directly in the gas streams.

To test the performance of the gas/Meissner-effect bearing, the test article was placed in an open dewar and liquid nitrogen was poured into the bottom of the dewar. Gas was supplied to the thrust bearing and turbine, and the shaft was spun up to approximately 500 revolutions per second (30,000 rpm). This speed was maintained by adjusting the throttle valve on the turbine supply as the gas cooled down.

The test article is cooled by two paths: convection from the turbine and thrust bearing gas, and conduction through the housing. The gas is cooled by passing through copper tubes located just below the housing. These tubes are immersed in liquid nitrogen. As the dewar is filled and the LN₂ level rises, the housing is cooled by boiling LN₂ on the bottom of the housing and on the brass base plate. In the initial cooldown tests, it was not possible to keep the shaft spinning at temperatures below approximately 150 K. This problem was traced to differential thermal expansion of the shaft and bearings.

At uniform temperatures, the gap between the bearing pads and the shaft is approximately 5 μm (0.0002 inches). The shaft diameter is 6.35 mm. The coefficient of thermal expansion of the shaft and bearing material (Tellurium Copper C14500) is 17.6 $\mu\text{m}/\text{m}/^\circ\text{C}$. A temperature difference between the shaft and bearing of 44°C is sufficient to reduce the shaft-bearing gap by half. A factor of two change in the bearing gap causes very large changes in the stiffness and drag of the bearing. If the gap closes sufficiently, the shaft will contact the bearings and stop.

The gap closed in these initial tests because the heat transfer to the body was more effective than heat transfer to the gas. Since the shaft was not in contact with the body, it stayed near the turbine and thrust bearing gas temperature. In the initial tests, temperature differences between the body and the shaft reached 50°C. After these tests, the test facility was modified to increase the effectiveness of heat transfer to the gas, and partially isolate the housing thermally from the LN₂.

After making these changes, the facility was cooled down to <85 K, slightly below the transition temperature of the superconductors (90-92 K). During the cooldown, heaters on the outside of the housing were used to maintain the housing warmer than the shaft. This ensured that the bearing gap would not close. During the cooldown, large changes in the shaft runout were observed as the gap changed due to differential expansion. When the shaft was 30°C colder than the housing, unstable half-speed whirl began when the shaft speed was 300 rps. As the temperature difference between the shaft and housing decreased, the half-speed whirl disappeared. At the coldest temperatures, near 85 K, the shaft showed marginal stability at 300 rps, with occasional large-amplitude excursions. Slowing the speed down to 100 rps stabilized the bearings.

A comparison of runout from two tests, one below the transition temperature (85 K) and one above (120 K), showed no significant differences between the two conditions. We conclude that for the configuration used in these tests, at temperatures near 77 K, the Meissner-effect did not contribute significantly to the stiffness and stability of the hybrid bearing.

4. CONCLUSIONS AND RECOMMENDATIONS

This project developed two innovative Meissner-effect radial bearings. The first of these uses permanent magnets and a small supply of pressurized gas to create a passive bearing system which can operate from room temperature to liquid helium temperature. The feasibility of this bearing concept was proven by analysis and experimental testing. While this concept is feasible, it does not appear practical for the very demanding miniature turbomachine application. The primary difficulties with the concept are the low bearing stiffness above the transition temperature, and the need for very precise alignment between the magnetic and mass centers of the bearing. The passive magnetic Meissner bearing could be useful in larger systems with more relaxed requirements for shaft runout. For these applications, the passive nature and low drag of the Meissner bearing could be quite attractive.

The second bearing concept appeared very promising, but was not demonstrated in practice. In this concept, the Meissner-effect was used to provide additional stiffness and damping to tilt-pad gas bearings at low temperature. Our tests indicated that for practical geometries, the Meissner-effect at temperatures near 80 K does not provide a significant improvement in gas bearing performance. At lower superconductor temperatures, the critical current density would be higher, and the Meissner-effect might contribute more strongly to the bearing stiffness and damping. Nonetheless, we do not recommend further development of this concept in light of the difficulties in maintaining proper shaft-bearing clearance during cooldown of the machine.

5. REFERENCES

- [1] Moon, F.C. et al., "Superconducting Rotating Assembly", U.S. Patent No, 4,886,778, Dec. 12, 1989.
- [2] Agarwala, A.K. " Electric Machinery Employing a Superconducting Element", International Patent Application Number PCT/US89/04165, Sept. 26, 1989.
- [3] Takahata, R., et al., "Characterization of Superconducting Magnetic Bearings", NASA CP-3152, Part 1, pp. 289-296, August 1991